HYSTERESIS MODELING OF Gd-films AND AFC-thin film RECORDING MEDIA

A. Ktena, D.I. Fotiadis, A. Berger and C.V. Massalas

06– 2003

Preprint, no 06 – 06 / 2003

Department of Computer Science
University of Ioannina
45110 Ioannina, Greece

Submitted on May 28, 2003

Hysteresis modeling of Gd-films and AFC- thin film recording media

A. Ktena[a], D.I. Fotiadis[a], A. Berger[b] and C.V. Massalas[c]

[a] Dept. of Computer Science, University of Ioannina, GR 45110 Ioannina, Greece
[b] Hitachi Global Storage Technologies, San Jose Research Center, San Jose, CA 95120, USA
[c] Dept. of Materials Science, University of Ioannina, GR 45110 Ioannina, Greece

ABSTRACT

This paper presents simulations of hysteresis processes in thin film media using 1D and 2D Preisach models. In the 2D version, a vector operator and superposition of angularly distributed models is used. The characteristic density of the material being modeled is reconstructed via a curve-fitting least-squares procedure that determines the parameters of a bivariate normal probability function density or a weighed mixture of normal densities based on major loop data only. The models have been identified for several samples of Gd-films annealed at various temperatures and AFC thin film recording media consisting of a hard and a soft phase antiferromagnetically coupled. The major and minor hysteresis loops calculated for all samples are in good agreement with experimental data.

Keywords: hysteresis modeling; minor loops; Preisach; AFC thin films; magnetic recording

Corresponding author: Prof. C.V. Massalas, Department of Materials Science, University of Ioannina, GR 45110 Ioannina, Greece, fax: 26510-97200, e-mail: cmasalas@cc.uoi.gr

1. Introduction

Hysteresis, defined as the rate independent memory effect [1], is the phenomenon where the current ouput state is a function of the current input as well as of past output extremum states. Ferromagnetic materials exhibit hysteresis in the magnetization response with respect to the applied field, $M(H)$; the magnetization, $M(t_0)$, for a given input field, $H(t_0)$, is a function of both $H(t_0)$ and past magnetization extremum values $M(t<t_0)$, thus behaving like a positive feedback mechanism [2]. Hysteresis is a desired effect, when the stability of information or energy storage is of interest as in the case of recording media or permanent magnets. Or, it can be an undesired effect when a material is used as a sensor or an actuator where hysteresis contributes to the uncertainty of the sensing or actuating element's response [3]. In either case, the modeling of hysteresis is highly desired and very challenging. A hysteresis model may be useful as core model in recording simulations [4] or finite element calculations of magnetic losses in laminations or real-time control in sensors or actuators. Such a model should be computationally efficient and adjustable to the material being modeled via a small number of parameters.The microscopic modeling of the network of short and long range interactions underlying the positive feedback mechanism of magnetic hysteresis leads to elaborate systems of equations requiring either cumbersome numerical calculations or simplifying assumptions particular to the type or geometry of the material or the application. The Preisach formalism, on the other hand, is a favorite in hysteresis modeling because of its abstract formulation and speed of the resulting calculations.

It postulates that hysteresis is the aggregate response of a distribution of elementary hysteresis operators. The hysteresis operator of the classical Preisach model (CPM) is a relay (Fig. 1a)

switching between two states, (+1, -1), at two critical input values, (a,b) where $a>b$. The probability density function $\rho(a,b)$ yielding the distribution of hysteresis operators at each output state is characteristic to the material being modeled and must be determined in order to identify the model. The resulting model is efficient and reliable for systems that fulfill certain necessary and sufficient conditions [2, 5]. The inherently scalar nature of the CPM can only allow for the one-dimensional (1D) treatment of a hysteresis process only which is not always valid since a lot of information is lost when modeling the 1D projection of a vector process. Furthermore, the magnetization response of a ferromagnetic material to an input field sequence contains, in general, a reversible component which cannot be reproduced by the CPM. To the extent that this reversible part can be attributed to the reversible rotation of the magnetization vector, one should expect that a vector formulation of the CPM would address both issues. One approach to vector hysteresis modeling is to superimpose the responses of angularly distributed CPMs [2]. However, this model fails to accurately reproduce the rotational properties of magnetic materials [6]. Alternatively, the original formalism can be extended to two dimensions by replacing the 1D operator (Fig. 1a) by a 2D operator (Figs. 1b, 1c) possessing both switching and rotational properties and superimposing the responses of angularly distributed models to account for the easy axes dispersion [4-6].

In the scalar case, the characteristic density of the material can be extracted from a set of detailed measurements [2]. This identification method cannot be extended to the 2D model because of the coupling between longitudinal and transverse components of the response and therefore, alternative methods must be considered. The alternative approach, used in this work, is based on a major loop measurement and consists in determining the parameters of the probability density function chosen to model the material under consideration [4, 6-8]. This

method is also applicable to the 1D model and can be used whenever the set of the detailed measurements required for the identification cannot be obtained. It can also be used in the hysteresis modeling in materials and systems other than ferromagnetism, like shape memory alloys (SMAs) [8], magnetic SMAs or magnetostrictive materials, elastoplasticity or economics, regardless of the underlying hysteresis mechanism.

This work aspires to demonstrate the applicability of the 1D Preisach model and the 2D extension together with the aforementioned identification method in the case of thin film media using data from two different experiments and media: major loop data from Gd-films previously annealed at different temperatures and minor loop data from anti-ferromagnetically coupled (AFC) recording media. In the case of Gd- films, annealing improves the crystallographic order in the sample and the major loop characteristic is different after each subsequent annealing step [9]. In the case of AFC media, the reversal of the soft layer at various hard layer states results in loops with two very distinct parts [12]. The model, the hysteresis operators and the characteristic density are discussed in the following section. The modeling of the experimental data and the discussion of the results are presented in section 3. The treatment of hysteresis throughout this work is quasistatic assuming that the output is not affected by the input rate.

2. The model

According to the Preisach formalism, the magnetization $M(t)$ for an input field $H(t)$ can be calculated by the CPM:

$$M(t) = \iint_{a \geq b} \rho(a,b) \gamma_{ab} H(t) \, da db \qquad (1)$$

The local hysteresis operator, γ_{ab}, when operating on the input $H(t)$ yields the local magnetization state m_t:

$$m_t = \gamma_{ab} \circ H(t) = \min\{1, m_{t-1}\}, \text{ where } \gamma_{ab} = \begin{cases} +1, & H(t) > a \\ -1, & H(t) < b \end{cases} \qquad (2)$$

The operator behaves like a relay switching between ±1-states at the upper and lower switching fields a and b. The result is weighed by the probability density function (pdf) $\rho(a,b)$, characteristic of the material being modeled, to yield the overall magnetization response. Notice that fields a and b are not functions of position or in any way related to the geometry of a sample; they rather represent effective switching fields of particles or grains in the statistical sense and account for the coercive field as well as the effective interaction field experienced by a given grain or collection of grains or particles. Therefore, modeling the material by a distribution of switching fields a and b and integrating over all a and b the global response is obtained [2].

The CPM formulation described in Eq. (1) is scalar and can model only irreversible processes. The reversible component of the response can be added on at the post-processing stage. The reversible processes in ferromagnetic materials are in general due to the reversible displacement of domain walls or the reversible rotation of the magnetization vectors aligned at an angle to the field direction. In order to model vector processes a 2D model must be used. As it turns out, the vector model accommodates the reversible component of the response as well.

According to the 2D formulation used in this work, the magnetization response $\mathbf{M}(t)$ to a vector input field $\mathbf{H}(t)$ is given by:

$$\mathbf{M}(t) = \int_{\substack{film \\ plane}} g(\theta) d\theta \iint_{a \geq b} \rho(a,b) \gamma_{ab} \mathbf{H}(t) da db \qquad (3)$$

The local hysteresis operator of the CPM is replaced by a vector operator able to respond to vector inputs and predict reversible rotation as well. The vector operator is based on the Stoner-Wohlfarth model (sw) depicted in Fig. 1b. It results from the minimization of the free energy equation of an ellipsoidal magnetic particle with uniaxial anisotropy under a normalized vector field $\mathbf{h}$. The astroid shape is the locus of the equation $h_x^{2/3} + h_y^{2/3} = 1$ where h_x and h_y are the components of the field along the easy and the hard axis of the particle, respectively. The magnetization angle ϕ with respect to the easy axis of the astroid is given by: $h_x \tan\phi - h_y + \sin\phi = 0$ and is the tangent to the astroid passing from the tip of the input vector. Switching occurs only if, during the transition from $m(t-1)$ to $m(t)$, the magnetization vector crosses the astroid from the inside out. Otherwise, the magnetization vector rotates reversibly. Introducing the first order approximation to the astroid, $h_x + h_y = 1$, the diamond shaped vector operator (dm) depicted in Fig. 1c is obtained. The dm-operator uses a similar hysteresis mechanism, it is computationally more efficient but does not have the physical attributes of the sw-operator. For inputs along the easy axis *x*, the two vector operators respond identically to the scalar operator of Fig. 1a. Fig. 2 shows a simulated experiment comparing the rotational properties of the two vector operators. The magnetization angle is calculated for several fields of constant normalized magnitude rotating 2π rad. For small inputs, the response is practically identical. As the input increases but not enough to cause switching, the sw-astroid rotates easier than the diamond. For large inputs, the sw-astroid allows for more switching.

Eq. (3) describes a 2D-model for a perfectly oriented system. That is, the easy axes of the operators all lie along the same orientation direction. The effect of orientation dispersion is

modeled by superimposing the responses of perfectly oriented models normally distributed according to a normal pdf $g(\theta)$ [6].

The density $\rho(a,b)$ is generated by a bivariate normal pdf or a weighed mixture of them [10]:

$$\rho(a,b) = w_1\left(\rho_1(a,b)\right) + w_2\left(\rho_2(a,b)\right) + \ldots \qquad \text{where } \sum_i w_i = 1, \tag{4}$$

in order to reproduce more complicated pdf shapes. The mixture of pdfs is appropriate for magnetic materials with more than one phase.

In order to identify the model decribed by (3) for a given material, the parameters of $\rho(a,b)$, namely the means μ_a and μ_b, and variances σ_a^2 and σ_b^2 of variables a and b, their correlation coefficient r, and the parameters of $g(\theta)$, μ_θ and σ_θ^2, must be determined. This can be accomplished by feeding a major loop data array to a least-squares based curve-fitting routine.

3. Results and Discussion

The model described in Section 2 has been used to model data from two different types of magnetic thin films. The first set of data is a set of major loops measured in Gd-films previously annealed at different temperatures. Annealing improves the crystallographic order and sharpens the anisotropy distribution of the sample [9], which is reflected in the phenomenology of the major ascending curves shown in Fig. 3. At higher annealing temperatures the loop is square and can be modeled by the CPM while at lower annealing temperatures, the anisotropy distribution width is larger than the threshold value at which the correlation of the magnetic reversal in the sample breaks down [11] and the loops are less square. In this case, the 2D model with a vector operator, *i.e.* the sw-operator, must be used. A KxK array is used for the bivariate density

$\rho(a,b)$ where K is the model discretization constant. Because of the loop symmetry, $M(H) = -M(-H)$, $\rho(a,b)$ is a normal pdf with means $\mu = \mu_a = \mu_b$, standard deviations $\sigma = \sigma_a = \sigma_b$, and correlation coefficient $r=0$. In the case of the vector model, the orientation dispersion density is centered at 0 and has a standard deviation σ_θ. Table 1 summarizes the results of the least squares fitting procedure for the ascending curves measured on Gd-film samples annealed at 610 °K and 560 °K prior to the hysteresis measurement. Notice that the same identification routine was used with both the 1D and the 2D model. In both cases, the only data fed to the algorithm were a dozen major loop data points. The relative error between experimental and calculated loops was 3.2% for the 610 °K curve (1D model/cpm operator) and 2.5 % for the 560 °K curve (2D model/sw-operator).

The second set of data is a set of minor loops measured in AFC layered media. Three layers are grown on a glass substrate and an underlayer: a soft magnetic layer is antiferromagnetically coupled to a hard magnetic layered through a Ru interlayer with no magnetic moment. The soft layer magnetization is reversed at different conditions of the hard layer and the resulting loops consist of two quite distinct parts which suggest that a weighed sum of two normal pdfs must be used to generate $\rho(a,b)$ (Eq. 4). In this case, the 2D model with the dm-operator is used. Again, only major loop data points are used in the fitting routine determining the weighing factor, w_1, with $w_2 = 1 - w_1$, the means μ_1 and μ_2 and standard deviations σ_1 and σ_2 of the symmetric pdfs ρ_1 and ρ_2 respectively. The identification routine results for the AFC data for two different K-values are summarized in Table 2. As expected, the weighing factor w_1 and standard deviations σ_1 and σ_2 are the same for either value of K while μ_1 and μ_2 are adjusted accordingly. The experimental and theoretical curves are shown in Fig. 4. Notice that the minor loops were reproduced successfully at both high fields and fields around the coercivity.

The input to the identification routine for both the Gd-film and AFC cases is about a dozen of data points from a measured major ascending or descending loop – if the loop is symmetric – that can be obtained even on a simple B-H tracer [13]. Once the density parameters are determined, the response to any sequence of fields can be modeled provided dymanic effects can be ignored. Therefore, this identification routine can be also used in conjunction with the 1D model when detailed measurements of the density cannot be carried out.

Other density functions (lorentzian, sigma) were also tried but the normal density has yielded the best results. Furthermore, the weighed sum of normal densities allows the reconstruction of other densities and the tailoring of a major loop characteristic. The "dm"-operator performs in most cases just as well as the "sw"-operator and is therefore preferred over the latter one since it is computationally more efficient. The model, the operators, and the identification procedure were all implemented in MATLAB 5.0. A major loop calculation for 100 input values would need approximately between 10 and 200 seconds on a Pentium III PC. The efficiency of the computation depends on the discretization of the model (K-value), the choice of operator and the dimensionality of the model, e.g. the 1D model is the most efficient routine while the 2D model using the sw-operator results in the lengthiest calculation.

4. Conclusion

Hysteresis models based on the Preisach formalism have been used to model the hysteretic response of the magnetization in thin film media. Depending on the squareness of the major loop characetristic, the dimensionality (1D or 2D) of the model and the appropriate operator (scalar or vector) are first chosen. A bivariate normal pdf or a mixture of normal densities is used to generate the characteristic density. The mixture of densities is a good choice for media consisting of more than one phases. A least-squares fitting algorithm using data from an

experimental major loop is used to identify the model for a given material. This identification routine may be used with either 1D or 2D models thus avoiding the detailed measurements usually needed in the CPM identification. The model is able to reproduce hysteresis proceses regardless of the underlying microstructure as illustrated by the calculated major loop characteristics of the various Gd-film samples and the major and minor loops of the two-phase AFC recording media. The model is computationally efficient enough to be used as core hysteresis model in recording simulations or finite element calculations.

References

[1] A. Visintin, in: Differential Models of Hysteresis, (Springer, Berlin,1994) pp. 10-29.

[2] I. D. Mayergoyz, Mathematical Models of Hysteresis, Springer-Verlag, New York, 1991.

[3] E. Hristoforou, Meas. Sci. & Technol., 14 (2003) R15.

[4] A. Ktena and S. H. Charap, IEEE Trans. Magn., 29 (6) (1993) 3661.

[5] D. Mayergoyz, Phys. Rev. Lett., 56(15) (1986) 1518.

[6] S. H. Charap and A. Ktena, J. Appl. Phys., 73 (1993) 5818.

[7] A. Ktena, D. I. Fotiadis, P. D. Spanos and C. V. Massalas, Phys. B, 306(1-4) (2001) 84.

[8] A. Ktena, D. I. Fotiadis, P. D. Spanos, A. Berger and C. V. Massalas, Int. J. of Eng. Sci., 40(20), (2002) 2235.

[9] A. Berger, A. W. Pang and H. Hopster, Phys. Rev. B 52 (1995) 1078.

[10] A. Ktena, D. I. Fotiadis and C. V. Massalas, IEEE Trans. Magn., 36(6) (2000) 3926.

[11] A. Berger, A. Inomata, J. S. Jiang, J. E. Pearson, and S. D. Bader, Phys. Rev. Lett. 85 (2001) 4176.

[12] E.E. Fullerton, D.T. Margulies, M.E. Schabes, M. Carey, B. Gurney, A. Moser, M. Best, G. Zeltzer, K. Rubin, H. Rosen, Appl. Phys. Lett. 77 (2000) 3806.

[13] E. Hristoforou, H. Chiriac and V. Nagacevschi, Sensors & Actuators A, 76 (1999) 442.

Tables

Table 1: Gd-film density parameters

T (°C)	**560**	**610**
Model/op	2D/sw	1D/cpm
K	60	40
σ_θ	30°	N/A
μ	51.44	25.83
σ	2.80	0.48
% error	3.20	2.50

Table 2: AFC-film density parameters

K	**40**	**80**
σ_θ	50°	50°
μ_1	24.78	51.12
σ_1	0.36	0.3
μ_2	33.81	66.02
σ_2	2.33	2.63
w_1	0.39	0.39

List of Figure Captions

Fig. 1: Hysteresis operators: (a) cpm (1D) (b) sw (2D) and (c) dm (2D).

Fig. 2: Comparison of rotational properties of the two vector operators, "sw" and "dm".

Fig. 3: Gd-film: Experimental and calculated ascending curves at annealing temperatures 610 °K and 560 °K.

Fig. 4: AFC-film: Experimental and calculated major and minor loops.

FIGURES

Fig. 1

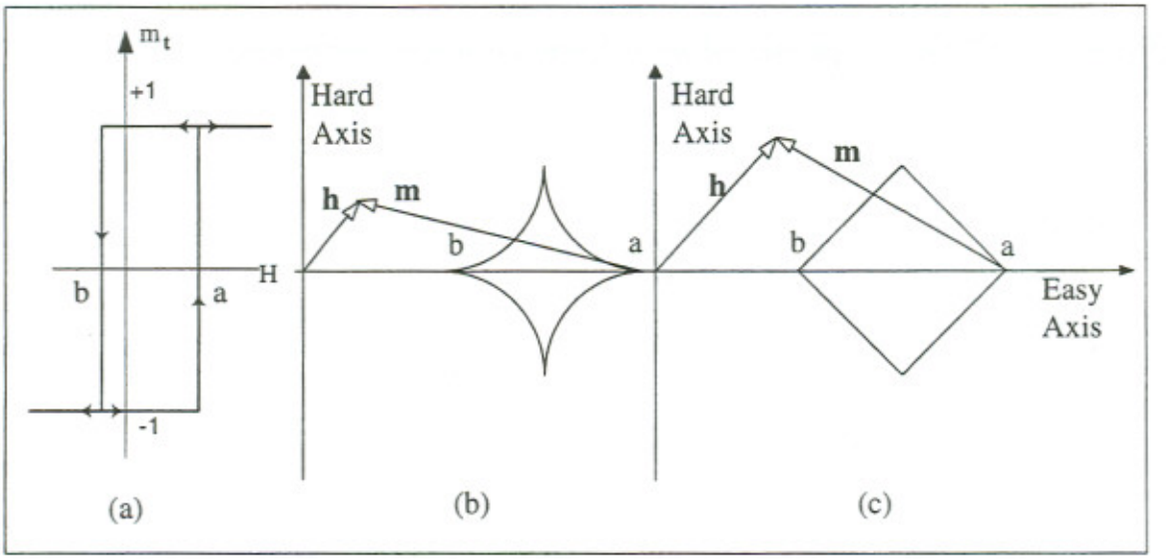

Fig. 2

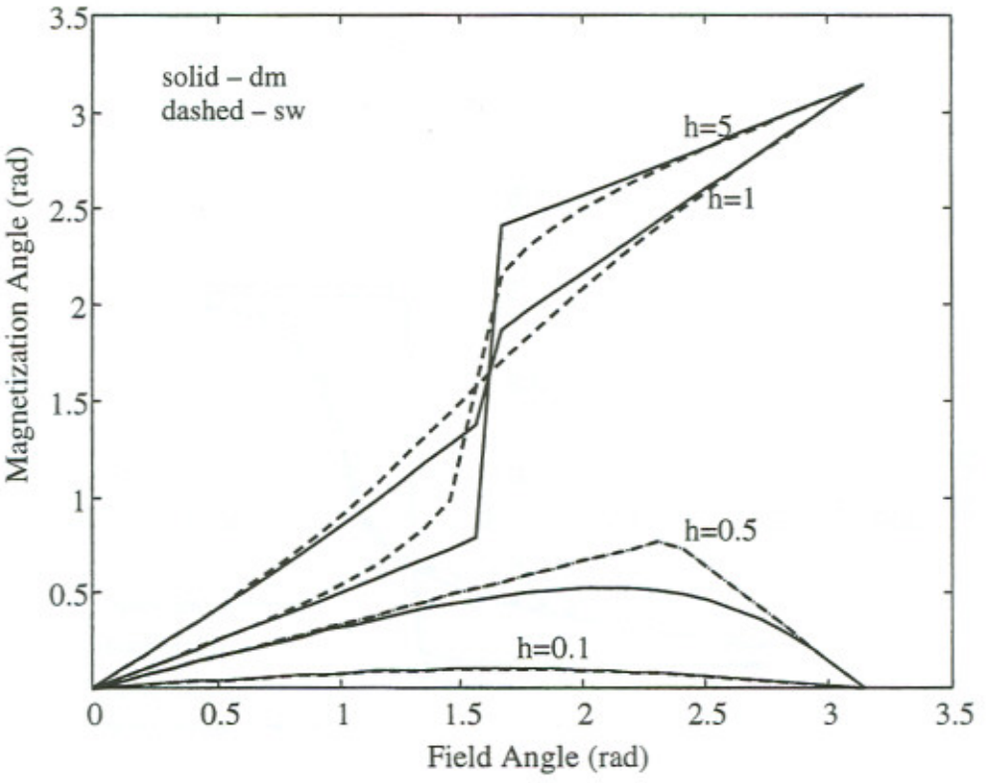
solid – dm
dashed – sw
h=5
h=1
h=0.5
h=0.1
Magnetization Angle (rad)
Field Angle (rad)
0
0.5
1
1.5
2
2.5
3
3.5

Fig. 3

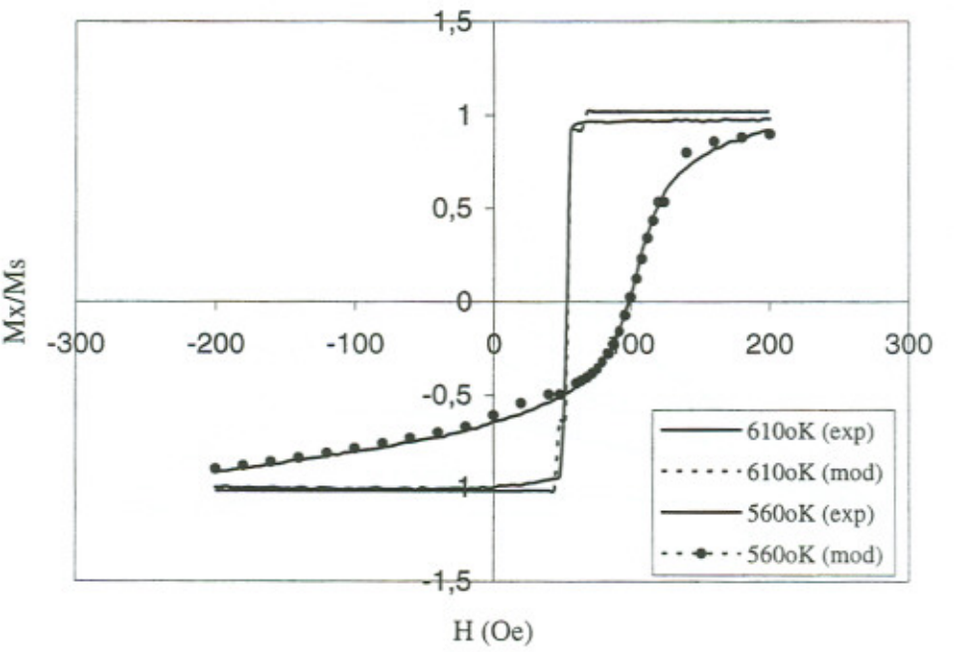
1,5
1
0,5
0
-0,5
-1
-1,5
-300
-200
-100
0
100
200
300
Mx/Ms
H (Oe)
610oK (exp)
610oK (mod)
560oK (exp)
560oK (mod)

Fig. 4

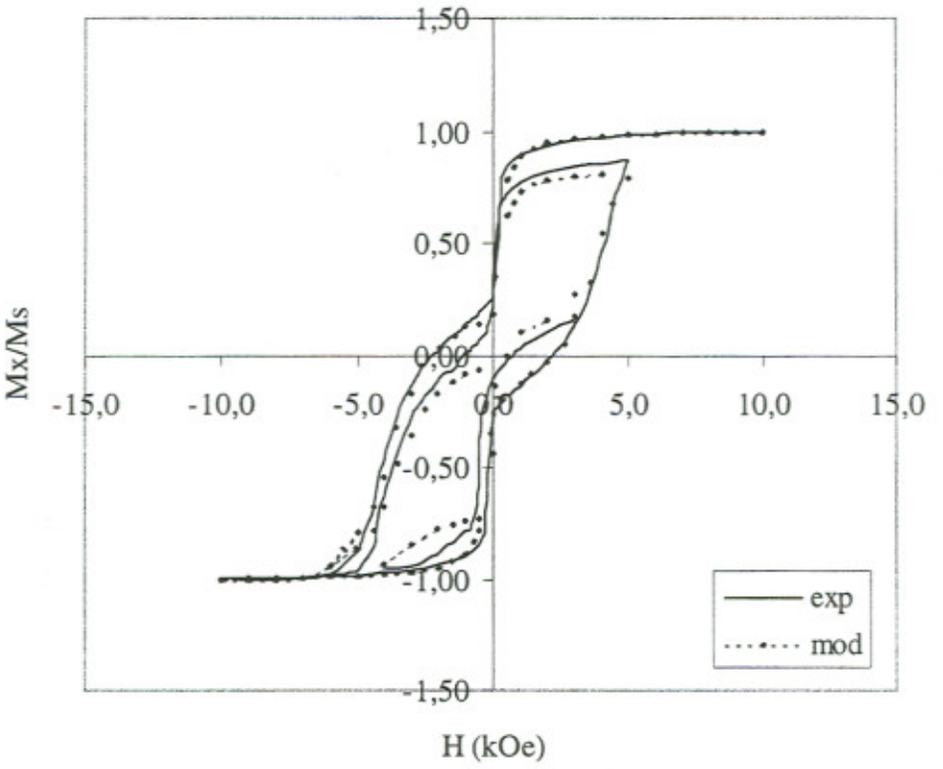
1,50
1,00
0,50
0,00
-0,50
-1,00
-1,50
-15,0
-10,0
-5,0
0,0
5,0
10,0
15,0
Mx/Ms
H (kOe)
exp
mod